Controllability and Observability of Temporal Hypergraphs

Anqi Dong, *Graduate Student Member, IEEE*, Xin Mao, Ram Vasudevan, *Senior Member, IEEE*, and Can Chen

***Abstract*—Numerous complex systems, such as those arisen in ecological networks, genomic contact networks, and social networks, exhibit higher-order and time-varying characteristics, which can be effectively modeled using temporal hypergraphs. However, analyzing and controlling temporal hypergraphs poses significant challenges due to their inherent time-varying and nonlinear nature, while most existing methods predominantly target static hypergraphs. In this letter, we generalize the notions of controllability and observability to temporal hypergraphs by leveraging tensor and nonlinear systems theory. Specifically, we establish tensor-based rank conditions to determine the weak controllability and observability of directed, weighted temporal hypergraphs. The proposed framework is further demonstrated with synthetic and real-world examples.**

***Index Terms*—Network analysis and control, networked control systems, time-varying systems, biological systems.**

I. Introduction

HYPERGRAPHS generalize graphs by allowing hyperedges to connect arbitrary subsets of nodes, capturing higher-order relationships unambiguously [1], [2]. Numerous real-world complex systems can be naturally represented using hypergraphs, including ecological networks, genomic contact networks, chemical reaction networks, co-authorship networks, and film actor/actress networks [3]. For instance, in ecological networks, species interactions often occur in higher-order combinations, where the relationship between two species can be influenced by one or more additional species [4], [5], [6].

Received 25 August 2024; revised 26 October 2024; accepted 12 November 2024. Date of publication 20 November 2024; date of current version 3 December 2024. Recommended by Senior Editor C. Briat. *(Anqi Dong and Xin Mao contributed equally to this work.) (Corresponding author: Can Chen.)*

Anqi Dong is with the Division of Decision and Control Systems and the Department of Mathematics, KTH Royal Institute of Technology, 100 44 Stockholm, Sweden (e-mail: anqid@kth.se).

Xin Mao is with the School of Data Science and Society, University of North Carolina at Chapel Hill, Chapel Hill, NC 27599 USA (e-mail: xinm@unc.edu).

Ram Vasudevan is with the Robotics Department, University of Michigan, Ann Arbor, MI 48109 USA (e-mail: ramv@umich.edu).

Can Chen is with the School of Data Science and Society and the Department of Mathematics, University of North Carolina at Chapel Hill, Chapel Hill, NC 27599 USA (e-mail: canc@unc.edu).

Digital Object Identifier 10.1109/LCSYS.2024.3504393

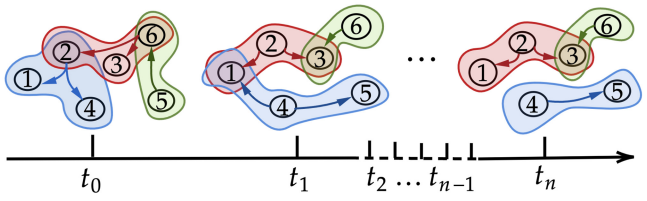

Fig. 1. Directed temporal hypergraph whose structure evolves over time. The connectivity is illustrated by hyperedges, represented as areas with distinct colors, and arrows indicating their directions.

Increasing evidence has revealed that higher-order interactions play a significant role in the dynamical processes of ecological networks [4]. Therefore, understanding the system-theoretic properties of hypergraphs such as controllability and observability becomes imperative for effectively managing and predicting the dynamics of complex systems.

A variety of results have been developed concerning the dynamics of static hypergraphs. For instance, Chen et al. [7] pioneered the development of a generalized Kalman's rank condition to determine the controllability of hypergraphs by leveraging homogeneous polynomial systems theory and tensor algebra, extending previous findings on graph controllability [8], [9]. Notably, the authors applied the rank condition to compute the minimum number of driver nodes of real-world hypergraphs. Subsequently, Pickard et al. [10], [11] employed a similar approach to investigate the weak observability of hypergraphs and the associated minimum number of sensor nodes. Recently, Zhang et al. [12] extended Pickard et al.'s work in a broader scope for hypergraph observability.

However, many real-world networks are time-varying and can be more accurately modeled using directed temporal hypergraphs, whose structure changes over time [13], [14], [15], [16] (see Fig. 1). As an illustrative example, in food webs, species interactions and predator-prey relationships are directional and exhibit seasonal fluctuations, such as changes in bird migration patterns affecting prey populations [17]. Moreover, these relationships can vary in response to environmental factors like temperature fluctuations, alterations in water flow patterns, and shifts in nutrient availability (e.g., warmer temperatures might favor certain fish species over others) [17]. Consequently, understanding these temporal variations is essential for studying system properties and designing optimal control strategies for food webs, which

has implications for species coexistence, biodiversity, and community persistence. Yet, most existing methods primarily focus on static hypergraphs, highlighting the need for the development of computational tools to analyze and control temporal hypergraphs.

In this letter, we aim to extend previous efforts on network controllability and observability to directed, weighted temporal hypergraphs by exploiting tensor theory and nonlinear systems theory. The key contributions are listed as follows:

- Building on [7], [18], we employ a tensor-based time-varying polynomial system model to capture the dynamics of directed, weighted temporal hypergraphs.
- We establish tensor-based rank conditions to determine the weak controllability and observability of time-varying polynomial systems and temporal hypergraphs.
- We demonstrate our framework with synthetic temporal hypergraphs and real-world ecological networks.

The article is organized into six sections. In Section II, we briefly review the notions of hypergraphs, tensor-based polynomial systems, and nonlinear controllability and observability. We derive tensor-based rank criteria to assess the weak controllability and observability of directed, weighted temporal hypergraphs in Sections III and IV, respectively. Two numerical examples are provided in Section V, and we conclude with future directions in Section VI.

II. Preliminaries

A. Hypergraphs

Hypergraphs generalize standard graphs by allowing hyperedges to connect more than two nodes. Mathematically, an undirected, unweighted hypergraph $\mathcal{G} = \{\mathcal{V}, \mathcal{E}\}$ where $\mathcal{V} = \{v_1, v_2, \ldots, v_n\}$ is the node set and $\mathcal{E} = \{e_1, e_2, \ldots, e_m\}$ is the hyperedge set such that $e_p \subseteq \mathcal{V}$ for $p = 1, 2, \ldots, m$ [1]. Two nodes are called adjacent if they belong to the same hyperedge. A hypergraph is called connected if, given two nodes, there is a path connecting them through hyperedges. The degree of a node is equal to the number of hyperedges that contain that node. If all hyperedges contain exactly k nodes, $\mathcal{G}$ is called a k-uniform hypergraph. Such hypergraphs can be represented as a kth-order, n-dimensional symmetric tensors [7]. Tensors are multidimensional arrays, generalized from vectors and matrices. The order of a tensor is the number of its dimensions, and each dimension is called a mode. An n-dimensional tensor is called symmetric if it is invariant under any permutation of its indices.

Definition 1 (Adjacency Tensors): Suppose that $\mathcal{G}$ is a k-uniform hypergraph with n nodes. The symmetric adjacency tensor $\mathcal{A} \in \mathbb{R}^{n\times n\times \overset{k}{\cdots} \times n}$ of $\mathcal{G}$ is defined as

$$\mathcal{A}_{i_1 i_2 \ldots i_k} = \begin{cases} 1/(k-1)! \text{ if } (i_1, i_2 \ldots, i_k) \in \mathcal{E} \\ 0 \qquad\qquad \text{otherwise} \end{cases}. \tag{1}$$

The definition can be generalized to weighted k-uniform hypergraphs by replacing $1/(k-1)!$ with a weight $w_{i_1 i_2 \ldots i_k}$. Moreover, directed hypergraphs can be addressed by treating each hyperedge as consisting of a tail set and a head set. For simplicity, we focus on directed hyperedges where the tail set contains a single node and the head set contains multiple nodes as in [18]. The corresponding adjacency tensor therefore becomes symmetric with respect to the last $k-1$ modes (referred to as almost symmetric [19], [20]), i.e., i_1 represents the tail and the rest of the indices represent the head. For non-uniform hypergraphs, we can represent them by combining adjacency tensors of different orders. A temporal hypergraph is a generalization of a (static) hypergraph that incorporates a time dimension [13], [14], making the adjacency tensors time-dependent, i.e., $\mathcal{A}_j(t)$ for $j = 2, 3, \ldots, k$, where k is the maximum cardinality of the hyperedges.

B. Tensor-Based Polynomial Systems

The dynamics of hypergraphs can be modeled using tensor-based polynomial systems [7], [12]. First, we introduce the operation of tensor matrix multiplications. Given a tensor $\mathcal{A} \in \mathbb{R}^{n\times n\times \overset{k}{\cdots} \times n}$, the tensor matrix multiplication $\mathcal{A} \times_p \mathbf{M}$ along mode p for a matrix $\mathbf{M} \in \mathbb{R}^{n\times m}$ is defined as

$$\left(\mathcal{A} \times_p \mathbf{M}\right)_{i_1 i_2 \ldots i_{p-1} j i_{p+1} \ldots i_k} = \sum_{i_p=1}^{n} \mathcal{A}_{i_1 i_2 \ldots i_k} \mathbf{M}_{i_p j}.$$

When $m = 1$, the definition reduces to the tensor vector multiplication. Analogous to graph dynamics with linear systems [8], the dynamics of a hypergraph can be naturally represented using tensors [7], [18].

Definition 2 (Hypergraph Dynamics): Suppose that $\mathcal{G}$ is a hypergraph with n nodes and maximum hyperedge cardinality k. The dynamics of $\mathcal{G}$ can be represented as

$$\dot{\mathbf{x}}(t) = \sum_{j=2}^{k} \mathcal{A}_j \times_2 \mathbf{x}(t) \times_3 \mathbf{x}(t) \times_4 \ldots \times_j \mathbf{x}(t), \tag{2}$$

where $\mathcal{A}_j \in \mathbb{R}^{n\times n\times \overset{j}{\cdots} \times n}$ are the jth-order adjacency tensors of $\mathcal{G}$ and $\mathbf{x}(t) \in \mathbb{R}^n$ represents the state of each node. For simplicity, we can rewrite (2) as $\dot{\mathbf{x}}(t) = \sum_{j=2}^{k} \mathcal{A}_j \mathbf{x}(t)^{j-1}$.

The tensor-based dynamical system (2) in fact belongs to the family of polynomial systems of degree $k-1$, which have been used to capture the dynamics of higher-order interactions in various fields [4], [21]. Similarly, the dynamics of a temporal hypergraph can be thus represented using a tensor-based time-varying polynomial system, i.e.,

$$\dot{\mathbf{x}}(t) = \sum_{j=2}^{k} \mathcal{A}_j(t) \mathbf{x}(t)^{j-1}, \tag{3}$$

where $\mathcal{A}_j(t)$ are the time-dependent jth-order adjacency tensors of the hypergraph. In this letter, $\mathcal{A}_j(t)$ can be weighted and almost symmetric, allowing for the modeling of directed, weighted temporal hypergraphs.

C. Nonlinear Controllability & Observability

Controllability and observability are two of the most fundamental system-theoretic properties of a dynamical system. Initially introduced for linear systems, both concepts can be verified using the classical Kalman's rank condition. However, defining and verifying the two properties becomes significantly more complex for nonlinear systems [22].

Definition 3 (Local Weak Controllability): A nonlinear control system is called locally weakly controllable at state $\mathbf{x}_0$ and time t_0 if, for any state $\mathbf{x}_1$ within a small neighborhood of $\mathbf{x}_0$, there exists a piecewise continuous control input that drives the system from $\mathbf{x}_0$ to $\mathbf{x}_1$ within a finite time interval.

Definition 4 (Local Weak Observability): A nonlinear output system is called locally weakly observable at state $\mathbf{x}_0$ and time t_0 if, there exists a neighborhood of $\mathbf{x}_0$ such that if two initial states $\mathbf{x}_0$ and $\mathbf{x}_1$ (within the neighborhood) produce indistinguishable outputs over a finite time interval, $\mathbf{x}_0 = \mathbf{x}_1$.

Weak controllability and observability refer to the cases when both definitions hold for any $\mathbf{x}_0 \in \mathbb{R}^n$ and $t_0 \in \mathbb{R}^+$. For nonlinear systems including homogeneous systems, many conditions have been established to determine local weak controllability and observability [23], [24].

III. Controllability

In this section, we propose a tensor-based rank condition for assessing the weak controllability of tensor-based polynomial time-varying systems of degree $k-1$ with linear inputs. The system is described by the following equation:

$$\dot{\mathbf{x}}(t) = \sum_{j=2}^{k} \mathcal{A}_j(t)\mathbf{x}(t)^{j-1} + \mathbf{B}(t)\mathbf{u}(t), \tag{4}$$

where $\mathcal{A}_j(t) \in \mathbb{R}^{n\times n\times \overset{j}{\cdots}\times n}$ are the jth-order time-dependent dynamic tensors, $\mathbf{B}(t) \in \mathbb{R}^{n\times m}$ is the time-dependent control matrix, and $\mathbf{u}(t) \in \mathbb{R}^m$ is the control input. Additionally, we introduce the operator of Lie brackets from differential geometry, which plays a crucial role in proving controllability. For more details of Lie brackets, we refer to [25].

Definition 5 (Lie Brackets): Given two vector fields $\mathbf{f}$ and $\mathbf{g}$, the Lie bracket of $\mathbf{f}$ and $\mathbf{g}$ at a point $\mathbf{x}$ is defined as

$$\big[\mathbf{f}, \mathbf{g}\big]_{\mathbf{x}} = \nabla\mathbf{g}(\mathbf{x})\mathbf{f}(\mathbf{x}) - \nabla\mathbf{f}(\mathbf{x})\mathbf{g}(\mathbf{x}),$$

where ∇ denotes the gradient operation.

A. Tensor-Based Rank Condition

We assume $\mathcal{A}_j(t)$ to be almost symmetric and weighted as they represent the adjacency tensors of directed, weighted temporal hypergraphs of different orders. We formulate the tensor-based controllability rank condition as follows, generalizing the classical Kalman's rank condition.

Proposition 1 (Controllability): The tensor-based polynomial time-varying control system (4) is locally weakly controllable at state $\mathbf{x}_0$ and time t_0 if and only if the state- and time-dependent controllability matrix defined as

$$\mathbf{C}(\mathbf{x}, t) = \big[\mathbf{M}_0(\mathbf{x}, t)\ \mathbf{M}_1(\mathbf{x}, t)\ \cdots\ \mathbf{M}_{n-1}(\mathbf{x}, t)\big], \tag{5}$$

where $\mathbf{M}_0(\mathbf{x}, t) = \mathbf{B}(t)$ and $\mathbf{M}_i(\mathbf{x}, t) = [\mathbf{\Omega}_1\ \cdots\ \mathbf{\Omega}_l\ \mathbf{\Delta}_1\ \cdots\ \mathbf{\Delta}_l]$ for $i = 1, 2, \ldots, n-1$, has full rank at $\mathbf{x} = \mathbf{x}_0$ and $t = t_0$. Here, l is the total number of columns of $\mathbf{M}_{i-1}(\mathbf{x}, t)$, $\mathbf{\Delta}_p = -\frac{\partial \mathbf{m}_{i-1}^{(p)}(\mathbf{x},t)}{\partial \mathbf{x}}\mathbf{B}(t)$, and

$$\mathbf{\Omega}_p = \sum_{j=2}^{k}(j-1)\mathcal{A}_j(t)\mathbf{x}^{j-2}\mathbf{m}_{i-1}^{(p)}(\mathbf{x}, t) - \frac{\partial \mathbf{m}_{i-1}^{(p)}(\mathbf{x}, t)}{\partial \mathbf{x}}\Big(\mathcal{A}_j(t)\mathbf{x}^{j-1}\Big) - \frac{\partial \mathbf{m}_{i-1}^{(p)}(\mathbf{x}, t)}{\partial t},$$

where $\mathbf{m}_{i-1}^{(p)}(\mathbf{x}, t)$ denotes the pth column of $\mathbf{M}_{i-1}(\mathbf{x}, t)$.

Proof: Based on nonlinear systems theory [23], [25], the controllability matrix (distribution) can be computed by recursively evaluating the Lie brackets of $\{\mathbf{B}(t), \sum_{j=2}^{k}\mathcal{A}_j(t)\mathbf{x}^{j-1}\}$, treating t as another state. Since $\mathcal{A}_j(t)$ are almost symmetric, for each iteration, it follows that

$$\mathbf{M}_i = \Big[\langle \mathbf{m}_{i-1}^{(1)}, \sum_{j=2}^{k}\mathcal{A}_j(t)\mathbf{x}^{j-1}\rangle_{\mathbf{x}}\ \ldots\ \langle \mathbf{m}_{i-1}^{(l)}, \sum_{j=2}^{k}\mathcal{A}_j(t)\mathbf{x}^{j-1}\rangle_{\mathbf{x}}\ \Big[\mathbf{m}_{i-1}^{(1)}, \mathbf{B}(t)\Big]_{\mathbf{x}}\ \ldots\ \Big[\mathbf{m}_{i-1}^{(l)}, \mathbf{B}(t)\Big]_{\mathbf{x}}\Big],$$

for some l, where $\langle \mathbf{f}, \mathbf{g}\rangle_{\mathbf{x}} = [\mathbf{f}, \mathbf{g}]_{\mathbf{x}} - \partial\mathbf{f}/\partial t$. Using the properties of tensor vector multiplications and Lie brackets, these brackets can be computed as

$$\langle \mathbf{m}_{i-1}^{(p)}, \sum_{j=2}^{k}\mathcal{A}_j(t)\mathbf{x}^{j-1}\rangle_{\mathbf{x}} = \mathbf{\Omega}_p \quad \text{and} \quad \Big[\mathbf{m}_{i-1}^{(p)}, \mathbf{B}(t)\Big]_{\mathbf{x}} = \mathbf{\Delta}_p.$$

The recursive process will converge at most $n-1$ steps based on the nonlinear controllability results in [26, Lemmas 1.8.1–1.8.3]. ■

The controllability matrix $\mathbf{C}(\mathbf{x}, t)$ (5) is in general state- and time-dependent. If the rank condition holds for all $\mathbf{x} = \mathbf{x}_0 \in \mathbb{R}^n$ and $t = t_0 \in \mathbb{R}^+$, the tensor-based time-varying polynomial system with linear inputs (4) is weakly controllable. Additionally, the condition present in Proposition 1 implies local strong accessibility which requires that the system can reach any state in a neighborhood of the initial state [25]. To compute the rank of the controllability matrix, we can utilize either numerical or symbolic computations. Numerical computations involve evaluating the controllability matrix at a finite number of sample points $(\mathbf{x}, t)$ and computing the rank using numerical rank operations. Symbolic computations entail expressing the entries of the controllability matrix as symbolic functions of $\mathbf{x}$ and t. By leveraging symbolic algebra software (e.g., MATLAB Symbolic Toolbox), we can perform exact calculations to determine the rank of the controllability matrix. However, symbolic computations can be computationally intensive and may struggle with the complexity for high-dimensional systems, potentially leading to errors.

Proposition 1 can be readily applied to the tensor-based polynomial time-varying control system (4) with symmetric $\mathcal{A}_j(t)$ for undirected temporal hypergraphs. Moreover, for k-uniform temporal hypergraphs (either directed or undirected) where the underlying dynamics is homogeneous of degree $k-1$, i.e., $j = k$ only in (4), we can obtain a simpler rank condition. In particular, when $k = 2$, it reduces to traditional temporal graphs with linear time-varying dynamics.

Corollary 1 (Homogeneous Case): The tensor-based homogeneous polynomial time-varying control system (4) (i.e., $j = k$ only) is locally weakly controllable at state $\mathbf{x}_0$ and

time t_0 if and only if the state-and time-dependent controllability matrix (5) with $\mathbf{M}_0(\mathbf{x},t) = \mathbf{B}(t)$ and $\mathbf{M}_i(\mathbf{x},t) = [\mathbf{\Omega}_1 \ \cdots \ \mathbf{\Omega}_l \ \mathbf{\Delta}_1 \ \cdots \mathbf{\Delta}_l]$ where $\mathbf{\Delta}_p = -\frac{\partial \mathbf{m}_{i-1}^{(p)}(\mathbf{x},t)}{\partial \mathbf{x}}\mathbf{B}(t)$ and

$$\mathbf{\Omega}_p = (k-1)\mathcal{A}_k(t)\mathbf{x}^{k-2}\mathbf{m}_{i-1}^{(p)}(\mathbf{x},t) - \frac{\partial \mathbf{m}_{i-1}^{(p)}(\mathbf{x},t)}{\partial \mathbf{x}}\left(\mathcal{A}_k(t)\mathbf{x}^{k-1}\right) - \frac{\partial \mathbf{m}_{i-1}^{(p)}(\mathbf{x},t)}{\partial t},$$

for $i = 1, 2, \ldots, n-1$, has full rank at $\mathbf{x} = \mathbf{x}_0$ and $t = t_0$.

Proof: Due to the bilinearity of Lie brackets, the result follows directly by eliminating the summation. ■

Corollary 2 (Linear Case): The linear time-varying control system (4) with $k = 2$ is weakly controllable at time t_0 if and only if the time-dependent controllability matrix (5) with $\mathbf{M}_0(t) = \mathbf{B}(t)$ and $\mathbf{M}_i(t) = \mathcal{A}_2(t)\mathbf{M}_{i-1}(t) - \frac{\partial \mathbf{M}_{i-1}(t)}{\partial t}$ for $i = 1, 2, \ldots, n-1$, has full rank at $t = t_0$.

Proof: The result follows by setting $k = 2$ in $\mathbf{M}_i(\mathbf{x},t)$ from Corollary 1, where it becomes state-independent. ■

Notably, the condition in Corollary 2 aligns with the controllability rank condition proposed in [27], which in fact can be used to establish full controllability for linear time-varying control systems.

B. Controllability of Temporal Hypergraphs

In network science, the notion of the minimum number of driver nodes (MNDN), introduced by Liu et al. [8], represents the smallest set of nodes necessary to fully control an entire network. This idea has broad applications, from understanding the behavior of biological systems to optimizing control strategies in social networks for disease prevention. By leveraging Proposition 1 and Corollary 1, we can discuss the weak controllability of directed, weighted temporal hypergraphs. Similar to the approach used in [7], we aim to identify the MNDN of a directed, weighted temporal hypergraph such that the corresponding controllability matrix of the underlying dynamics has full rank. The MNDN is a powerful concept that can be used to steer the dynamics of temporal hypergraphs with minimal effort [8]. It can also serve as an indication of the robustness of temporal hypergraphs [7]. Intuitively, if the MNDN of a temporal hypergraph is high, it will require more effort or energy to control the hypergraph or steer the underlying system. Furthermore, the MNDN provides insights into the underlying topology of the temporal hypergraph, which helps identify key nodes that play a crucial role in the system's dynamics. For simplicity, we assume that the control matrix is time-independent (i.e., $\mathbf{B}$) and each input can only be imposed on one node.

Identifying the MNDN through a brute-force search is NP-hard and time-consuming [7]. We offer a heuristic method for approximating the minimum subset of driver nodes in a directed, weighted temporal hypergraph, where nodes are selected based on the maximum change in the rank of the controllability matrix (Algorithm 1). The rank computations in Step 6 can be performed either numerically or symbolically. In Step 7, if multiple v^* are obtained, we can either pick one randomly or break the tie based on their degrees. Note that the final subset of driver nodes $\mathcal{D}$ is highly likely to be minimal (i.e., MNDN), but it is not guaranteed. Algorithm 1 can be applied at a fixed state and time to determine local weak controllability, and it can also be extended to varying states and times through symbolic computation.

Algorithm 1 Greedy Driver Nodes Selection

1: Given almost symmetric, weighted time-varying adjacency tensors $\mathcal{A}_j(t) \in \mathbb{R}^{n\times n\times \overset{j}{\cdots}\times n}$ of a temporal hypergraph
2: Let $\mathcal{V} = \{1, 2, \ldots, n\}$ and the index set $\mathcal{D} = \emptyset$
3: Let $\mathbf{C}_{\mathcal{D}}(\mathbf{x},t)$ be the controllability matrix with the control matrix formed from the index set $\mathcal{D}$
4: **while** $\text{rank}(\mathbf{C}_{\mathcal{D}}(\mathbf{x},t)) < n$ **do**
5: **for** $v \in \mathcal{V} \setminus \mathcal{D}$ **do**
6: Compute
$$\Delta(v) = \text{rank}\left(\mathbf{C}_{\mathcal{D}\cup\{v\}}(\mathbf{x},t)\right) - \text{rank}(\mathbf{C}_{\mathcal{D}}(\mathbf{x},t))$$
7: **end for**
8: Set $v^* = \text{argmax}_{v\in\mathcal{V}\setminus\mathcal{D}}\Delta(v)$
9: Set $\mathcal{D} = \mathcal{D}\cup\{v^*\}$
10: **end while**
11: **return** subset of driver nodes $\mathcal{D}$

IV. Observability

In this section, we propose a tensor-based rank condition for assessing the weak observability of tensor-based polynomial time-varying systems of degree $k-1$ with linear outputs, i.e.,

$$\begin{cases} \dot{\mathbf{x}}(t) = \sum_{j=2}^{k}\mathcal{A}_j(t)\mathbf{x}(t)^{j-1} \\ \mathbf{y}(t) = \mathbf{L}(t)\mathbf{x}(t) \end{cases}, \tag{6}$$

where $\mathbf{L}(t) \in \mathbb{R}^{q\times n}$ is the time-dependent output matrix, and $\mathbf{y} \in \mathbb{R}^q$ is the output. Again, we assume that $\mathcal{A}_j(t)$ are almost symmetric and weighted for modeling directed, weighted temporal hypergraphs. Additionally, we provide a brief review of the Lie derivative operator, which plays a crucial role in proving observability.

Definition 6 (Lie Derivatives): Given a vector field $\mathbf{f}$ and a scalar field h, the Lie derivative of h along $\mathbf{f}$ is defined as

$$\mathcal{L}_{\mathbf{f}}h = (\partial h/\partial \mathbf{x})\mathbf{f}.$$

Moreover, it satisfies

$$\mathcal{L}_{\mathbf{f}}Dh = D\mathcal{L}_{\mathbf{f}}h,$$

where D denotes the differential operator.

Detailed definitions and properties of Lie derivatives can be found in [25]. We formulate the tensor-based observability rank condition as follows.

Proposition 2 (Observability): The tensor-based polynomial time-varying output system (6) is locally weakly observable at state $\mathbf{x}_0$ and time t_0 if and only if the state- and time-dependent observability matrix defined as

$$\mathbf{O}(\mathbf{x},t) = \begin{pmatrix} \mathbf{N}_0(\mathbf{x},t) \\ \mathbf{N}_1(\mathbf{x},t) \\ \vdots \\ \mathbf{N}_{n-1}(\mathbf{x},t) \end{pmatrix}, \tag{7}$$

where $\mathbf{N}_0(\mathbf{x}, t) = D(\mathbf{L}(t)\mathbf{x})$, and

$$\mathbf{N}_i(\mathbf{x}, t) = \sum_{j=2}^{k} \frac{\partial \mathbf{N}_{i-1}(\mathbf{x}, t)}{\partial \mathbf{x}} \left(\mathcal{A}_j(t)\mathbf{x}^{j-1}\right) + \frac{\partial \mathbf{N}_{i-1}(\mathbf{x}, t)}{\partial t}$$

for $i = 1, 2, \ldots, n-1$, has full rank at $\mathbf{x} = \mathbf{x}_0$ and $t = t_0$.

Proof: Based on nonlinear systems theory [24], [25], the observability matrix (codistribution) can be computed by evaluating the Lie derivatives of the output along the system state, treating t as another state. Since $\mathcal{A}_j(t)$ are almost symmetric, for each iteration, it follows that

$$\mathbf{N}_i = \left[\tilde{\mathcal{L}}_{\sum_{j=2}^{k} \mathcal{A}_j(t)\mathbf{x}^{j-1}} \mathbf{n}_{i-1}^{(1)} \ \cdots \ \tilde{\mathcal{L}}_{\sum_{j=2}^{k} \mathcal{A}_j(t)\mathbf{x}^{j-1}} \mathbf{n}_{i-1}^{(l)}\right]^{\top},$$

where l is the total number of rows of $\mathbf{N}_{i-1}$, $\mathbf{n}_{i-1}^{(p)}$ is the pth row of $\mathbf{N}_{i-1}$, and $\tilde{\mathcal{L}}_{\mathbf{f}} h = \partial h/\partial t + (\partial h/\partial \mathbf{x})\mathbf{f}$. Using the properties of tensor vector multiplications and Lie derivatives, each element can be computed as

$$\tilde{\mathcal{L}}_{\sum_{j=2}^{k} \mathcal{A}_j(t)\mathbf{x}^{j-1}} \mathbf{n}_{i-1}^{(p)} = \sum_{j=2}^{k} \frac{\partial \mathbf{n}_{i-1}^{(p)}}{\partial \mathbf{x}} \left(\mathcal{A}_j(t)\mathbf{x}^{j-1}\right) + \frac{\partial \mathbf{n}_{i-1}^{(p)}}{\partial t}.$$

For example, $\mathbf{N}_1(\mathbf{x}, t)$ can be computed as

$$\mathbf{N}_1(\mathbf{x}, t) = D\left(\sum_{j=2}^{k} \mathbf{L}(t)\left(\mathcal{A}_j(t)\mathbf{x}^{j-1}\right) + \frac{\partial(\mathbf{L}(t)\mathbf{x})}{\partial t}\right).$$

The recursive process will converge at most $n-1$ steps due to the nonlinear observability results in [26, Lemmas 1.9.1, 1.9.2, and 1.9.6]. ■

Similar to the controllability matrix, the observability matrix $\mathbf{O}(\mathbf{x}, t)$ (7) is in general state- and time-dependent. If the rank condition holds for all $\mathbf{x} = \mathbf{x}_0 \in \mathbb{R}^n$ and $t = t_0 \in \mathbb{R}^+$, the tensor-based time-varying polynomial system with linear outputs (6) is weakly observable. For k-uniform temporal hypergraphs (either directed or undirected), we can drop the summation in $\mathbf{N}_i(\mathbf{x}, t)$.

Corollary 3 (Homogeneous Case): The tensor-based homogeneous polynomial time-varying output system (6) (i.e., $j = k$ only) is locally weakly observable at state x_0 and time t_0 if and only if the state- and time-dependent observability matrix (7) with $\mathbf{N}_0(\mathbf{x}, t) = D(\mathbf{L}(t)\mathbf{x})$, and

$$\mathbf{N}_i(\mathbf{x}, t) = \frac{\partial \mathbf{N}_{i-1}(\mathbf{x}, t)}{\partial \mathbf{x}} \mathcal{A}_k(t)\mathbf{x}^{k-1} + \frac{\partial \mathbf{N}_{i-1}(\mathbf{x}, t)}{\partial t},$$

for $i = 1, 2, \ldots, n-1$, has full rank at $\mathbf{x} = \mathbf{x}_0$ and $t = t_0$.

Corollary 4 (Linear Case): The linear time-varying output system (6) with $k = 2$ is weakly observable at tiem t_0 if and only if the time-dependent observability matrix (7) with $\mathbf{N}_0(t) = \mathbf{L}(t)$ and $\mathbf{N}_i(t) = \mathbf{N}_{i-1}(t)\mathcal{A}_2(t) + \frac{d\mathbf{N}_{i-1}(t)}{dt}$, for $i = 1, 2, \ldots, n-1$, has full rank at $t = t_0$.

The criterion above coincides with the observability rank condition proposed in [27], which in fact can be used to establish full observability for linear time-varying output systems. Based on Proposition 2 and Corollary 3, we can discuss the weak observability of directed, weighted temporal hypergraphs. Specifically, we are interested in identifying the minimum number of sensor nodes (MNSN) required for a directed, weighted temporal hypergraph to ensure that the associated observability matrix has full rank. The MNSN is a critical notion that enables the reconstruction of the full internal state of a temporal hypergraph [28]. Additionally, it is essential for designing feedback control, relying on estimations of the plant state based solely on the plant output or the measurements collected from its sensors [10]. For simplicity, we assume that the output matrix is time-independent (i.e., $\mathbf{L}$) and each output can only be imposed on one node. Therefore, we can utilize an approach similar to Algorithm 1 to find the "minimum" set of sensor nodes of a directed, weighted temporal hypergraph.

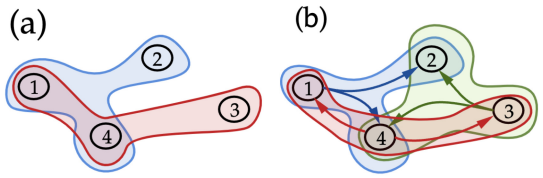

Fig. 2. 3-uniform temporal hypergraphs without (a) and with (b) directed hyperedges.

V. Numerical Examples

We illustrate our framework with two numerical examples, focusing on the controllability of temporal hypergraphs. All computations were performed using MATLAB R2022b with the Symbolic Toolbox. The associated code can be found at https://github.com/dytroshut/temp.graph.

A. Uniform Temporal Hypergraphs

In this example, we constructed two synthetic 3-uniform temporal hypergraph with 4 nodes. The first is undirected, containing hyperedges $e_1 = \{v_1, v_2, v_4\}$ and $e_2 = \{v_1, v_3, v_4\}$ with weights $\mathcal{A}_{124} = 2t$ and $\mathcal{A}_{134} = -t$ (the same weights are assigned to their permutations), as shown in Fig. 2(a). The control matrix for this hypergraph is defined as $\mathbf{B}_1(t) = [0, 1/t, t, 0]$. The second hypergraph is directed, containing hyperedges $e_1 = \{v_1, v_2, v_4\}$, $e_2 = \{v_4, v_1, v_3\}$, and $e_3 = \{v_2, v_3, v_4\}$, with weights $\mathcal{A}_{124} = \mathcal{A}_{142} = t^2$, $\mathcal{A}_{413} = \mathcal{A}_{431} = 2t$, and $\mathcal{A}_{324} = \mathcal{A}_{342} = 1/t$, as shown in Fig. 2(b). The control matrix for this hypergraph is defined as $\mathbf{B}_2(t) = [2t, 1/t, t, t^2]$. We computed the controllability matrices $\mathbf{C}_1$ and $\mathbf{C}_2$ for both hypergraphs based on Corollary 1. The results show that $\text{rank}(\mathbf{C}_1) = 3$ and $\text{rank}(\mathbf{C}_2) = 4$, using symbolic computation. Consequently, the first hypergraph is not weakly controllable with the control matrix $\mathbf{B}_1(t)$, while the second hypergraph is weakly controllable with $\mathbf{B}_2(t)$.

B. Higher-Order Ecological Systems

In ecological networks, species interactions are often time-varying and involve higher-order combinations. Understanding these interactions is crucial for accurately modeling ecosystem dynamics and predicting the impact of changes within the network. In our second example, we considered two temporal ecological networks with pairwise or third-order interactions among seven species $\mathcal{S} = \{s_1, s_2, \ldots, s_7\}$ (see Fig. 3). The first network (a) involves pairwise interactions $\{s_2, s_5\}$ and $\{s_3, s_6\}$

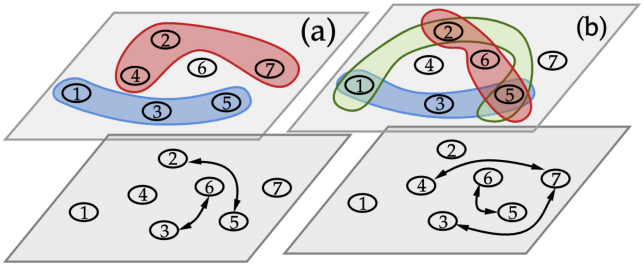

Fig. 3. Two higher-order temporal ecological networks with pairwise and third-order interactions.

and third-order interactions $\{s_1, s_3, s_5\}$ and $\{s_2, s_4, s_7\}$. The second network (b) consists of pairwise interactions $\{s_3, s_7\}$, $\{s_4, s_7\}$, and $\{s_5, s_6\}$ and third-order interactions $\{s_1, s_3, s_5\}$, $\{s_2, s_5, s_6\}$, and $\{s_1, s_2, s_5\}$.

To determine the MNDN for both temporal hypergraphs, we followed the updating scheme outlined in Algorithm 1, assuming that the control matrices are time-independent indicating the driver nodes. Therefore, the estimated MNDN of the two ecological networks can be computed as $\mathcal{D}_1 = \{s_1, s_2, s_4\}$ and $\mathcal{D}_2 = \{s_3, s_7\}$, implying that the former ecological network structure is more robust to external inputs than the latter. Note that the MNDN may not be unique. For instance, in the case of the second ecological network, alternative possible choices of MNDN include $\mathcal{D}_2 = \{s_1, s_3\}$.

VI. Conclusion

In this letter, we extended the framework of controllability and observability to directed, weighted temporal hypergraphs. By leveraging tensor and nonlinear systems theory, we developed novel tensor-based rank conditions to assess the weak controllability and observability of temporal hypergraphs. We further demonstrated the practical relevance and effectiveness of our approach using a synthetic example and real-world ecological networks. Incorporating temporal dynamics in complex systems provides new insights and computational tools for analyzing and controlling complex dynamics in time-varying higher-order networks. In the future, it would be valuable to explore stronger controllability and observability conditions for temporal hypergraphs and to apply this framework to large-scale, real-world hypergraph data (e.g., how to efficiently evaluate the symbolic rank for large-scale temporal hypergraphs?). Additionally, investigating optimal control design for temporal hypergraphs presents an important direction for further research. This could have significant implications for areas such as network stability, resource allocation, and dynamic behavior prediction in complex systems.

References

[1] C. Bergh, *Hypergraphs: Combinatorics of Finite Sets*, vol. 45. Amsterdam, The Netherlands, Elsevier, 1984.

[2] Y. Gao, Z. Zhang, H. Lin, X. Zhao, S. Du, and C. Zou, "Hypergraph learning: Methods and practices," *IEEE Trans. Pattern Anal. Mach. Intell.*, vol. 44, no. 5, pp. 2548–2566, May 2022.

[3] C. Chen and Y.-Y. Liu, "A survey on hyperlink prediction," *IEEE Trans. Neural Netw. Learn. Syst.*, vol. 35, no. 11, pp. 15034–15050, Nov. 2024.

[4] E. Bairey, E. D. Kelsic, and R. Kishony, "High-order species interactions shape ecosystem diversity," *Nat. Commun.*, vol. 7, no. 1, 2016, Art. no. 12285.

[5] S. Cui, Q. Zhao, G. Zhang, H. Jardón-Kojakhmetov, and M. Cao, "On the analysis of a higher-order Lotka-Volterra model: An application of S-tensors and the polynomial complementarity problem," 2024, *arXiv:2405.18333*.

[6] P. Singh and G. Baruah, "Higher order interactions and species coexistence," *Theor. Ecol.*, vol. 14, no. 1, pp. 71–83, 2021.

[7] C. Chen, A. Surana, A. M. Bloch, and I. Rajapakse, "Controllability of hypergraphs," *IEEE Trans. Netw. Sci. Eng.*, vol. 8, no. 2, pp. 1646–1657, Apr.–Jun. 2021.

[8] Y.-Y. Liu, J.-J. Slotine, and A.-L. Barabási, "Controllability of complex networks," *Nature*, vol. 473, no. 7346, pp. 167–173, 2011.

[9] G. Duan, A. Li, T. Meng, G. Zhang, and L. Wang, "Energy cost for controlling complex networks with linear dynamics," *Phys. Rev. E, Stat. Phys. Plasmas Fluids Relat. Interdiscip. Top.*, vol. 99, no. 5, 2019, Art. no. 52305.

[10] J. Pickard, A. Surana, A. Bloch, and I. Rajapakse, "Observability of hypergraphs," in *Proc. 62nd IEEE Conf. Decision Control (CDC)*, 2023, pp. 2445–2451.

[11] J. Pickard, C. Stansbury, A. Surana, I. Rajapakse, and A. Bloch, "Geometric aspects of observability of hypergraphs," 2024, *arXiv:2404.07480*.

[12] C. Zhang, H. Yang, S. Cui, B. Jiang, and M. Cao, "Global and local observability of hypergraphs," 2024, *arXiv:2405.18969*.

[13] L. Neuhäuser, R. Lambiotte, and M. T. Schaub, "Consensus dynamics on temporal hypergraphs," *Phys. Rev. E, Stat. Phys. Plasmas Fluids Relat. Interdiscip. Top.*, vol. 104, no. 6, 2021, Art. no. 64305.

[14] A. Myers, C. Joslyn, B. Kay, E. Purvine, G. Roek, and M. Shapiro, "Topological analysis of temporal hypergraphs," in *Proc. Int. Workshop Algorithms Models Web-Graph*, 2023, pp. 127–146.

[15] A. Li, S. P. Cornelius, Y.-Y. Liu, L. Wang, and A.-L. Barabási, "The fundamental advantages of temporal networks," *Science*, vol. 358, no. 6366, pp. 1042–1046, 2017.

[16] T. Qin, G. Duan, and A. Li, "Detecting the driver nodes of temporal networks," *New J. Phys.*, vol. 25, no. 8, 2023, Art. no. 83031.

[17] K. Schoenly and J. E. Cohen, "Temporal variation in food Web structure: 16 empirical cases," *Ecol. Monogr.*, vol. 61, no. 3, pp. 267–298, 1991.

[18] S. Cui, G. Zhang, H. Jardón-Kojakhmetov, and M. Cao, "On Metzler positive systems on hypergraphs," 2024, *arXiv:2401.03652*.

[19] C. Chen, "Explicit solutions and stability properties of homogeneous polynomial dynamical systems," *IEEE Trans. Autom. Control*, vol. 68, no. 8, pp. 4962–4969, Aug. 2023.

[20] L. Liang, S. Cui, and F. Liu, "Discrete-time SIS social contagion processes on hypergraphs," 2024, *arXiv:2408.08602*.

[21] K. Fujarewicz, M. Kimmel, and A. Swierniak, "On fitting of mathematical models of cell signaling pathways using adjoint systems," *Math. Biosci. Eng.*, vol. 2, no. 3, pp. 527–534, 2005.

[22] R. Hermann and A. Krener, "Nonlinear controllability and observability," *IEEE Trans. Autom. Control*, vol. 22, no. 5, pp. 728–740, Oct. 1977.

[23] A. Martinelli, "Rank conditions for observability and controllability for time-varying nonlinear systems," 2020, *arXiv:2003.09721*.

[24] A. Martinelli, "Extension of the observability rank condition to time-varying nonlinear systems," *IEEE Trans. Autom. Control*, vol. 67, no. 9, pp. 5002–5008, Sep. 2022.

[25] A. M. Bloch, *Nonholonomic Mechanics*. New York, NY, USA: Springer, 2015.

[26] A. Isidori, *Nonlinear Control Systems*. London, U.K.: Springer, 1985.

[27] L. M. Silverman and H. E. Meadows, "Controllability and observability in time-variable linear systems," *SIAM J. Control*, vol. 5, no. 1, pp. 64–73, 1967.

[28] Y.-Y. Liu, J.-J. Slotine, and A.-L. Barabási, "Observability of complex systems," in *Proc. Nat. Acad. Sci.*, vol. 110, no. 7, pp. 2460–2465, 2013.